Archives of Acoustics Vol. **48**, No. 1, pp. 93–101 (2023), doi: 10.24425/aoa.2022.142908

Research Paper

Airborne and Structure-Borne Noise Control in the MB Truck Cabin Interior by the Noise Reduction in the Transmission Path

Nader MOHAMMADI

Department of Mechanical Engineering, Islamic Azad University, Parand Branch
Tehran, Iran; e-mail: nader.mohammadi@gmail.com; nmohamady@ut.ac.ir

(*received May 20, 2022; accepted September 9, 2022*)

In the current study, investigations are made to control the MB truck cabin interior noise by reducing noise in the transmission path. The main sources of cabin noise include the engine, exhaust system, air inlet system, driveline system, and tyres (especially at higher speeds). Furthermore, vibrations of the body and interior parts of the truck may significantly impact the overall in-cabin sound level. Noise is transmitted into the cabin via air (airborne noise) and cabin structure (structure-borne noise). In the noise treatment phase, noise transmission paths are considered. A viscoelastic layer damping material is used to reduce the vibration amplitude of the cabin back wall. The overall loss factor and vibration amplitude reduction ratio for the structure treated is calculated. Computational results are then compared with the values obtained by the experimental modal analysis results. Choosing the suitable material and thickness can significantly reduce the vibration amplitude. A sound barrier, silicon adhesive, and foam are also utilised for noise control in the transmission path. The effectiveness of the mentioned acoustic materials on cabin noise reduction is evaluated experimentally. The experimental SPL values are reported in the frequency range of 20 Hz–20 kHz based on a 1/3 octave filter. The experimental results show that using acoustics materials reduces the overall in-cabin sound level for a wide range of frequencies.

Keywords: truck noise sources; airborne noise; structure-borne noise; acoustic materials; viscoelastic layer damping; modal analysis.

1. Introduction

Unwanted sound or noise has some undesired impacts on human conversations. They can be as strong as to cause a person hearing loss or hearing impairments. Today, noise pollution is among those problems on which widespread efforts are focused to attenuate its effects. A low noise level is an essential feature of a product indicating its quality. Many companies, including car manufacturers, implement widespread attempts to improve their products' quality by reducing the levels of noise. Among other noise sources, vehicle noise (especially those generated by heavy trucks) significantly contributes to noise pollution. As car manufacturing industries developed and advanced, creating a competitive environment among them, the importance of vehicle quality and comfort has become more notable. A vehicle's interior and exterior noise and vibration level are essential factors determining its quality. In a vehicle, unwanted sounds and vibrations hurt vehicle parts and can cause additional dynamic loads, fatigue, and loss of power, thus reducing the vehicles efficiency. Also, vehicle sounds and vibrations may significantly affect the passengers' comfort. Sound is a part of a structure vibrational energy transmitted to its surrounding environment. Therefore, there is a direct relationship between sound and vibration.

Mohanty *et al.* (2000) used a CAE method for noise reduction in a truck cabin interior. The finite element (FE) and the boundary element method (BEM) were used to characterize the acoustic field of a truck cabin interior in terms of the natural frequencies and the mode shapes. Structural vibration responses of the cabin were computed for excitations at the cabin mounts in the frequency range from 50 to 250 Hz. Interior noise levels at the driver's right ear were determined using the boundary element method for excitations at the cabin mounts. A panel acoustic contribution analysis (PACA) was done to determine the structural areas of the cabin contributing most to the noise levels at the driver's right ear. Structure-borne noise was reduced in the cabin's interior by selecting and placing sound absorbing material at the appropriate locations in the cabin, as determined by PACA.

Li *et al.* (2008) employed active noise control methods to control the noise of the heavy truck's cabin interior. An interior noise field test for the heavy truck was performed, and frequencies of interior noise of this vehicle were analysed. Then the least squares lattice (LSL) algorithm was used as the signal processing algorithm of the controller, and a closed-loop control DSP system was developed. The residual signal at the driver's ear was used as a feedback signal. Lastly, the developed active noise control (ANC) system was loaded into the heavy truck cabin, and controlling the noise at the driver's ear for that truck at different driving speeds was attempted.

Antila *et al.* (2008) simulated an ANC system using noise data measured in a truck cabin. The data were treated in the simulation process with a control system model. The result was evaluated both numerically and by listening tests. The possible benefits of the proposed ANC system included less fatigue for driver and co-driver, no need for excessive noise insulation in the truck, and more comfortable driving conditions. The challenges in designing the system were its complexity, reliability, and potentially high price. These pros and cons were discussed in the paper, and a concept of the system realisation was given.

Bealko (2009) examined noise exposure inside haul truck cabins experienced during a typical workday with normal operator practices, the effect of noise-reduction features inside the cabin, and the consequence of disabling noise controls (unnecessary open doors/windows), and the significance of haul truck and cabin maintenance factors.

Lu *et al.* (2013) studied an adaptive active noise control (AANC) system of the interior truck cabin to reduce low-frequency noise. A normalisation Fractional Least Mean Square (FLMS) algorithm Simulink model was established in MATLAB/Simulink. Then taking it as the core, a feedforward adaptive active control system and a feedback adaptive active control system of the interior tuck cabin were established in MATLAB/Simulink. Considering the actual channel error effects on systems, the noise reduction effects of two adaptive active control systems were verified from the simulation results. Comparing the two adaptive active control systems showed that the feedforward adaptive active control system was more stable than the other one.

Ang *et al.* (2016) provided an overview of the existing industrial practices used for cabin noise control in various industries such as automotive, marine, aerospace, and defense. The current industrial practices pertaining to cabin noise control were discussed. Also, the potential of acoustic metamaterials was highlighted.

Saxena and Jadhav (2021) measured the interior noise and vibration on one of the light trucks, and a few dominant low-frequency noise booms were observed in the operation range. Modal analysis was done for the cabin at virtual and experimental levels, and a few modes were found close to these noise booms. Vibrations were measured across the cabin mounts, and it was found that the isolation of front mounts is not effective at lower frequencies. The mount design was modified to shift the natural frequency and improve the isolation behaviour at the lowest dominant frequency. Also, the interior noise and vibration measurement was carried out on the truck fitted with selected mounts, and substantial vibration, overall noise reduction, and drastic boom noise reduction were achieved.

Herein, the main cabin noise sources are investigated for an MB truck, including both vibrations and acoustic noises. Viscoelastic damping layers are employed to control vibration, while sound barriers, silicon adhesive, and foam are used to control noise. The effect of viscoelastic damping layers on the vibration amplitude of the cabin back wall is studied both theoretically and experimentally. Also, the impact of acoustic materials on cabin noise attenuation is experimentally investigated.

2. Main sources of cabin noise in an MB truck

Preliminary investigations indicate that the main sources of noise in an MB truck (including acoustic noise as well as vibration) can be categorised as follows:

- power system including engine, air inlet system, and exhaust system,
- driveline system including gearbox, driveshaft, and differential,
- tyre/road interaction.

The main sources of interior noise (the cabin noise) are the power system, driveline system, and tyre/road interactions. However, the noise generated by tyre/road interaction dominates the driveline system noise at speeds exceeding 80 km/h (Johnson, 1996).

2.1. Engine

The engine is the main source of interior noise in trucks. The engine vibration and engine noise are studied in the following sections (Taylor, 1982; SAE, 1992).

2.1.1. Engine vibration

The inertia of the engine's moving parts and the cylinder pressure changes create forces that cause engine components' movement. As a result, vibration with variable frequency and amplitude covers the motor's whole structure, and it is called internal vibration. Internal engine vibration includes the flexural and torsional vibration of the crankshaft, the piston's torsional vibration, and the auxiliary systems such as the oil pump, water pump, and turbocharger. Continuous systems such as crankcase and crankshaft housing, pipes and tubes such as oil pipelines and exhaust have an important role in the internal vibration of the engine. The high-frequency vibration (noise) from combustion and gears involvement is also important (Taylor, 1982; SAE, 1992).

2.1.2. Engine noise

Engine noise includes mechanical, combustion, fuel injection, air inlet, and exhaust system noise (Taylor, 1982; Harris, 1991; Beranek, 1992).

Diesel engines have higher pressure rise rates than spark ignition engines, indicating higher importance of combustion noise in diesel engines than that in spark ignitions engines. The acoustic and vibrational properties of the parts related to the combustion phenomenon play an important role in the amount of combustion noise. Today, research shows that the most important noise in diesel engines is combustion noise. Experimental research shows that 106 BTU/hr of heat released by combustion can generate about 29 W of acoustic power (equivalent to a sound power level of 135 dB) (Taylor, 1982; Harris, 1991).

Exhaust in internal combustion engines is one of the main sources of noise. Noise is caused by the periodic release of gases from the exhaust manifold (Harris, 1991).

2.2. Driveline system

The driveline system in trucks has a more intense effect on the overall noise level than in passenger cars and should be considered. Driveline system noise includes gearbox, driveshaft, and differential noise. The differential noise has minor effects on the overall noise level (SAE, 1992).

2.3. Tyre/road noise

Since the speed of the truck is generally less than 80 km/h, the effect of the tyre/road on the cabin noise is less important (Johnson, 1996).

3. Noise and vibration control

The noise (including acoustic noise and vibration) control methods have been categorised into three categories: noise control at the source, noise control in the transmission path, and noise control at the receiver. This study considers the transmission path for both noise and vibration. In other words, the cabin noise is controlled in its transmission paths. The sound from different sources is transmitted into the cabin via air (airborne sound transmission) and structure (structure-borne sound transmission). Figure 1 shows principal noise sources and their transmission paths to the cabin. Also, Fig. 2 shows structure-borne and airborne paths of noise transmission to the cabin.

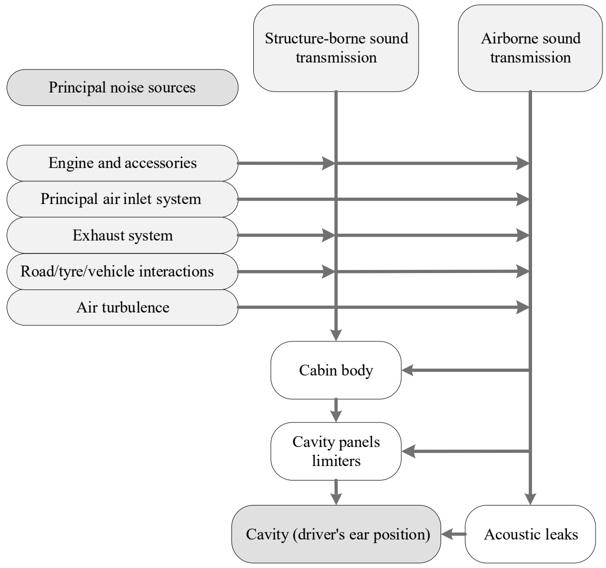

Fig. 1. Principal noise sources and their transmission paths to the cabin.

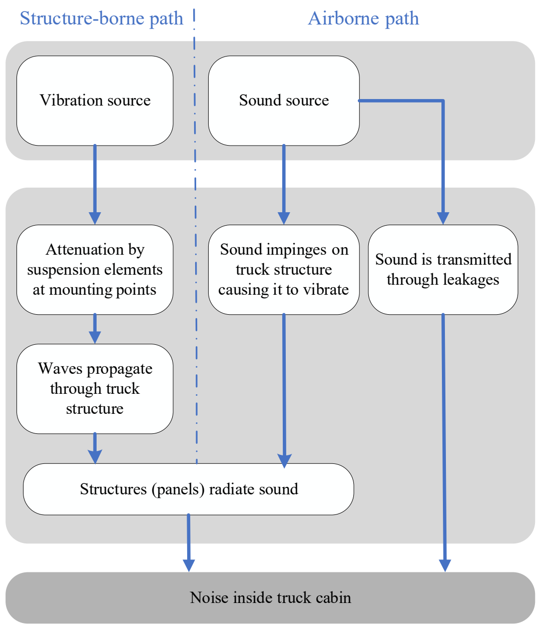

Fig. 2. Structure-borne and airborne paths of noise transmission to the cabin.

3.1. Vibration

In many machines, excited vibrations cover a wide range of frequencies. In this case, the conventional method of vibration control, i.e., separation of the natural frequencies of the system from the excitation frequencies, is not possible. While dynamic vibration absorbers are not used in such a situation because it is possible to excite several natural modes, viscoelastic layer damping treatment is applied to control the vibration of a structure. Such layers reduce the structural vibration amplitude by energy dissipation, causing the overall noise level to be lower (Pujara, 1992; Barber, 1992). A layer damping can be used to control the vibration of the truck cabin, engine housing, cylinder head cover, and crankcase.

Researchers have studied two types of viscoelastic damping treatments: unconstrained layer damping (UCLD) treatment and constrained layer damping (CLD) treatment. Unconstrained layer (free layer) treatments are widely used in the automotive industry as additional layers on large sheet metal panels. The elongation between the supporting metallic and the viscoelastic due to the bending of supporting plates in the low-frequency range introduces the material damping. In the constrained layer treatments, a viscoelastic layer is placed between the vibrating structure and a solid plate (usually metal). In this method, most of the vibrational energy is lost due to the shear deformation of the viscoelastic layer (Jones, 1985; Nashif *et al.*, 1985; Malik, 1990). In this study, the unconstrained layer damping treatment is used.

The overall loss factor η_s of the structure treated can be obtained by Eq. (1) (Jones, 1985):

$$\eta_s = \frac{\eta_D}{1 + A/(Be)}, \tag{1}$$

where

$$A = \frac{(1 - n^2 e)^3 + [1 + (2n + n^2)e]^3}{(1 + ne)^3},$$

$$B = \frac{(1 + 2n + n^2 e)^3 - (1 - n^2 e)^3}{(1 + ne)^3},$$

$$n = h_D/h, \qquad e = E_D/E,$$

and where h is the thickness of the structure, h_D is the thickness of the layer damping, E is the Young modulus of the structure, E_D is the real part of the complex modulus of the layer damping, η_D is the loss factor of the layer damping, and η_s is the overall loss factor of the structure treated.

3.2. Noise

Sound barriers are used to block the transmission of airborne sound by providing mass to existing structures or hung as limp mass partitions. The performance of a sound barrier is measured in terms of its transmission loss (TL). In practical applications, the value of TL for a sound barrier is often expressed as the mass law: the more the surface density of a sound barrier, the higher its TL. Herein, a sound barrier, silicon adhesives, and foam are used to control noise.

4. Treatment and results

The engine, the exhaust system, and the air inlet system are the main sources of cabin noise in the MB truck. Figure 3 shows the MB truck cabin, the main sources of interior noise, and their transmission paths into the cabin. Engine noise is transmitted into the cabin by the air (airborne noise: A) through acoustic leaks and the cabin body (floor and firewall), and by the cabin structure (structure-borne noise: S) through the floor and the firewall. The exhaust system noise is transmitted into the cabin by the air through acoustic leaks and the floor, and by the cabin structure through the floor and back wall. The air inlet system noise is transmitted into the cabin by the air through acoustic leaks and firewall, and by the cabin structure through the firewall.

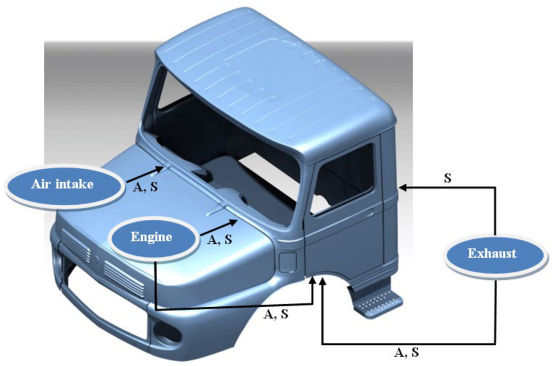

Fig. 3. MB truck cabin, its main sources of interior noise, and their transmission paths into the cabin.

Here, a viscoelastic layer damping is used on the back wall to control vibration, and acoustic materials are used on the floor and the firewall to control noise.

4.1. Viscoelastic damping layer

4.1.1. Theoretical model

A viscoelastic layer damping is used here to control vibration. The back wall vibration is considered and treated. A suitable viscoelastic material is selected, and the overall loss factor and the ratio of vibration amplitude reduction are calculated for the structure treated (back wall with viscoelastic layer installed).

The behaviour of viscoelastic materials is a function of temperature and frequency. First, the structure's operating temperature range and vibration frequency range (back wall) must be determined. Then, the material with the maximum value $E_D\eta_D$ is selected in that temperature and frequency range. The temperature of the back wall varies in the range of 35–45°C, and the structure's natural frequencies are calculated to determine the frequency range of the back wall vibration.

The truck's cabin is designed such that its back wall is nearly a flat surface. So, the back wall can be appropriately modelled as a rectangular sheet. The natural frequencies of a rectangular sheet are calculated as follows (Pujara, 1992):

$$\omega_{pq} = \pi^2 \sqrt{\frac{gD}{\rho h}\left[\left(\frac{p}{a}\right)^2 + \left(\frac{q}{b}\right)^2\right]}, \tag{2}$$

where $D = Eh^3/[12(1-\nu^2)]$, a, b, and h are length, width, and thickness of the sheet, respectively, ρ, E, and ν are density, Young modulus, and Poisson's ratio of the plate, respectively, g is the gravitational acceleration, and ω_{pq} are the natural frequencies of a rectangular sheet.

The back wall plate in the MB truck is made of USt 37-2, and its dimensions and properties are listed in Table 1. From Eq. (2), natural frequencies corresponding to the back wall are presented in Table 2.

Table 1. Dimensions and physical and mechanical properties of the back wall plate in the MB truck.

a [m]	b [m]	h [m]	ρ [kg/m^3]	E [GPa]	ν	D
1.96	1.45	1.5×10^{-3}	7850	210	0.3	64.9

Table 2. Natural frequencies of the back wall.

f_{11} [Hz]	f_{12} [Hz]	f_{21} [Hz]	f_{22} [Hz]	f_{23} [Hz]	f_{32} [Hz]
10	17	14	19.8	26.7	23.8

From Table 2, the frequency range of the back wall vibration 10–25 Hz is considered. According to the temperature and frequency range, LD-400 viscoelastic material is selected as the most suitable material, as it has the highest $E_D\eta_D$ value over the mentioned temperature and frequency ranges. In Table 3, the E_D, η_D, and $E_D\eta_D$ values are tabulated for frequencies of 10, 15, 20, and 25 Hz and temperatures of 35, 40, and 45°C. The density of the viscoelastic layers is $\rho_D = 1500$ kg/m^2.

Table 3. Properties of the LD-400 viscoelastic layer damping (AFML data).

Frequency [Hz]	T [°C]	η_D	E_D [GPa]	$E_D\eta_D$
10	35	0.512	1.2986	0.6649
	40	0.443	1.0517	0.4660
	45	0.413	0.8648	0.3572
15	35	0.521	1.4213	0.7405
	40	0.463	1.1691	0.5413
	45	0.412	0.9607	0.3958
20	35	0.529	1.4828	0.7844
	40	0.471	1.2041	0.5671
	45	0.418	0.9903	0.4139

The overall loss factor can be calculated by Eq. (1). The E_D and η_D values are extracted from Table 3. Here, the temperature and frequency are equal to 40°C and 10 Hz (the first natural frequency). Table 4 presents the overall loss factor of the structure treated for n = 2, 4, 6, and 10.

Table 4. Overall loss factor of the structure treated.

n	2	4	6	8	10
η_s	0.1034	0.2812	0.3653	0.3921	0.4062

Assuming that the first mode of vibration is important, the structure treated is modelled as a simple one degree of freedom system. Values of the vibration amplitude reduction ratio of the structure are computed as follows (Malik, 1990):

$$\frac{X}{Y} = \left[\frac{1+(2\xi r)^2}{(1-r^2)^2+(2\xi r)^2}\right]^{1/2}, \tag{3}$$

where X/Y represents the ratio of vibration amplitude reduction, r is the frequency ratio, and ξ is the damping ratio equal to $\eta_s/2$ (Malik, 1990). Figure 4 shows the values of X/Y for n = 2, 4, 6, and 10.

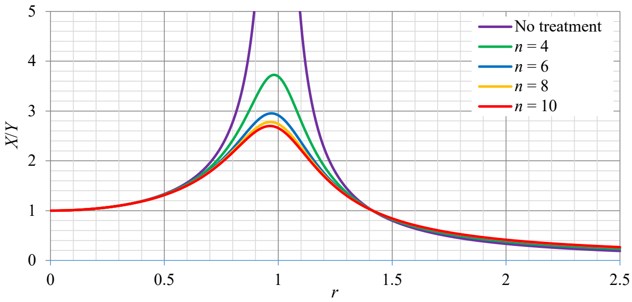

Fig. 4. Ratio of the vibration amplitude reduction for the structure treated.

4.1.2. Experimental work

In order to calculate the vibration amplitude, the structure is excited, and the acceleration response is obtained. A stringer that has been installed on the head of a shaker (B&K Type 4808) does the excitation; a force transducer (Endevco Model 2311-100) on the head of the shaker, and an accelerometer (Endevco Model 65-100) are used to sense the input and output of the system, respectively. A signal analyser (B&K Type 3560-B), a power amplifier (B&K Type 2719), and a PC equipped with PULSE 8 software were utilised for data acquisition and signal processing. Figure 5 shows a schematic sketch of the experimental setup used for the measurements.

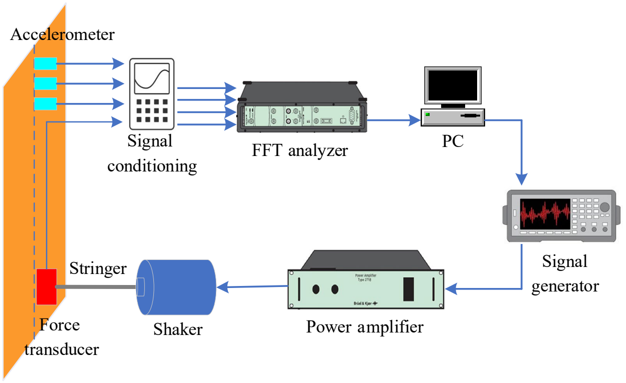

Fig. 5. Schematic sketch of the experimental setup used for the measurements.

First, natural frequencies of the structure are measured. In Table 5, the experimental and theoretical values of the natural frequency are shown. Then, the vibration amplitude of the structure is determined before and after the treatment. The excitation frequency is normalised with respect to the first natural frequency. Figure 6 shows experimental and theoretical values of the ratio of the vibration amplitude reduction for the structure treated for $n = 4$.

Table 5. Natural frequencies of the back wall.

Mode number	f_{11} [Hz]	f_{12} [Hz]	f_{21} [Hz]	f_{22} [Hz]	f_{23} [Hz]	f_{32} [Hz]
Theoretical	10	17	14	19.8	26.7	23.8
Experimental	9.5	16.1	13.2	18.7	25.1	22.8

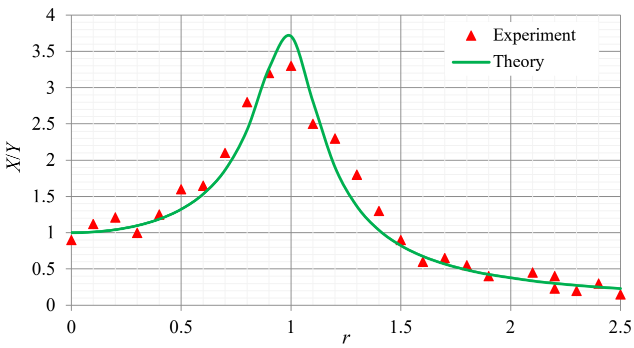

Fig. 6. Experimental and theoretical values of the ratio of the vibration amplitude reduction for the structure treated, $n = 4$.

4.2. Acoustic materials

Herein, acoustic materials, including sound barrier, Silicon adhesives, and polyurethane foam are used. Rubber sheets, namely "Genaral seal & Panchari", made in Iran, are used as a sound barrier on the floor and firewall. This material has a density of 5 kg/m^2, with its TL_E values presented in Table 6. These values are obtained by testing a squared specimen with an area of 900 cm^2. Also, the TL_M values calculated by mass law are shown in Table 6.

Table 6. TL values corresponding to mass law (TL_M) and testing (TL_E) of the sound barrier.

Frequency [Hz]	TL [dB]	
	Experimental	Mass law
125	14	9
250	16	15
500	22	21
1000	26	27
2000	27	33
4000	30	39
8000	36	45

Silicone adhesives are here used in tape and liquid forms. The silicone tape is used on the floor and firewall, and the liquid silicone is used to treat leakages of the structure. Also, polyurethane foam is injected into the side member and other noise transmission paths.

4.2.1. Experimental work and results

The experiments are performed according to standards ISO 5128 (1980) and SAE-J336 (2011). Figure 7 shows a schematic sketch of the experimental setup used for the measurements. In addition to the shown equipment, a loudspeaker is used as an external noise source.

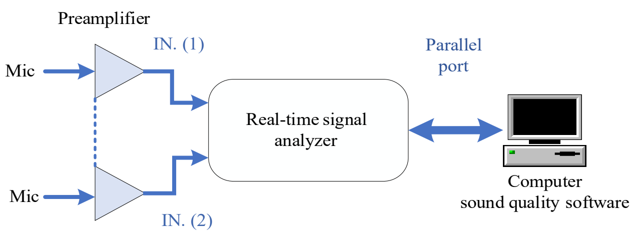

Fig. 7. Schematic sketch of the experimental setup used for the measurements.

Herein, a B&K 4155 1/2 free-field microphone is used. The noise level measured inside the cabin changes drastically with the microphone's position, and the microphone must be able to accurately describe the noise sensed by the driver and his/her assistant. The microphone's position is determined via ISO 5128 (see Fig. 8). A Norsonic microphone calibrator type 1251 is used for calibration. Also, a Norsonic preamplifier type 1201 is used here. A four-channel signal analyser (B&K Type 3560-C) and a PC equipped with PULSE 8 software are utilised for data acquisition and signal processing.

The test placement must be a place with minimum background noise and distance from direct noise sources and reflective surfaces exceeding 15 m. The

Fig. 8. Position of the microphone inside the cabin.

background noise level will be measured separately and subtracted from the overall noise level in places where the background noise level is high.

Three tests, including the loudspeaker, engine, and road, are performed in 6 steps. In the loudspeaker test, the engine is turned off, and a loudspeaker is used as the noise source. The loudspeaker is a Norsonic reference sound source with a weighted sound power output: 94 dB re 1 pW (50 Hz line frequency). The loudspeaker is located 1.1 m from the front axle on the centreline of the two axles. In the engine test, the engine is operating at a speed of 1500 rpm for 5–10 seconds (the truck is stationary). In the road test, the truck runs 200 m at a constant speed of 30 km/h in 3rd gear. The 6 test steps are:

Step 1: Performing loudspeaker, engine, and road tests before any treatment.

Step 2: Performing loudspeaker and engine tests after removing the carpet from the cabin floor.

Step 3: Performing engine and loudspeaker tests once the sound barrier and silicon adhesives cover the firewall leaks.

Step 4: Performing loudspeaker and engine tests once the sound barrier covers the floor.

Step 5: Performing the road test after all leaks and the floor are covered by the sound barrier and silicon adhesives.

Step 6: Performing the road test after complete treatment, including the coverage of all leaks in the floor and firewall by the sound barrier and silicon adhesive, and foam injection into the side member.

The test results are shown in Figs. 9 to 15. The experimental SPL values are reported in the frequency range of 20 Hz–20 kHz based on a 1/3 octave filter. Figure 9 shows the measured sound pressure level (SPL) inside the cabin for the loudspeaker test (steps 2 and 3). Knowing that the structure rather than the air transmits low-frequency sound waves (compared to high-frequency sound waves), one may see that coverage of leaks does not affect the noise level reduction for frequencies lower than 1000 Hz. The maximum noise

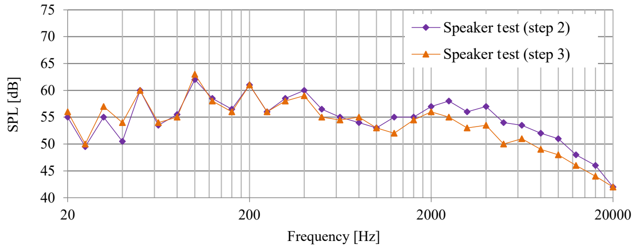

Fig. 9. Measured SPL inside the cabin; the loudspeaker test (steps 2 and 3).

reduction of 4 dB is seen at 5000 Hz. In addition, the carpet has little impact on cabin noise reduction.

Figure 10 shows the measured SPL inside the cabin for the loudspeaker test (steps 2 and 4). Coverage of the cabin floor with the sound barrier reduces the cabin noise level for frequencies higher than 1000 Hz (a maximum of 6 dB at 5000 Hz).

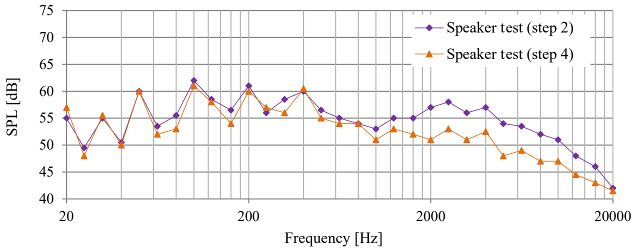

Fig. 10. Measured SPL inside the cabin; the loudspeaker test (steps 2 and 4).

According to Fig. 11, the cabin carpet has very small contribution to the sound pressure level inside the cabin (a maximum of 2 dB at 2500 Hz).

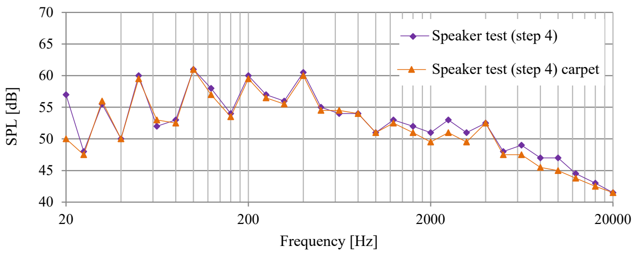

Fig. 11. Impact of the carpet on the SPL inside the cabin.

Figure 12 shows the measured SPL inside the cabin for the engine test (steps 1 and 3). The results indicate

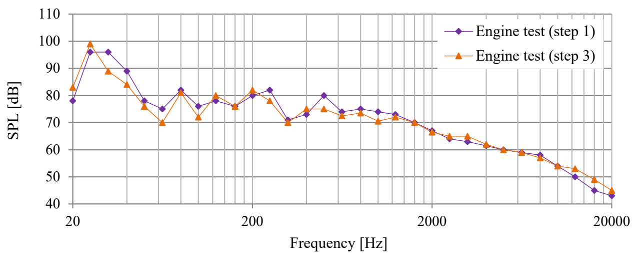

Fig. 12. Measured SPL inside the cabin; the engine test (steps 1 and 3).

that even when all the leaks are entirely covered, the engine noise is transmitted into the cabin by the structure itself (structure-borne noise).

Figure 13 shows the measured SPL inside the cabin for the engine test (steps 1 and 2). The impact of the cabin carpet on the cabin noise attenuation is significant for the frequencies higher than 1000 Hz. An average reduction of 13 dB is observed in the SPL inside the cabin. However, the carpet does not affect the cabin noise reduction for the frequencies lower than 1000 Hz. In this frequency range, the engine noise is transmitted into the cabin by the structure itself.

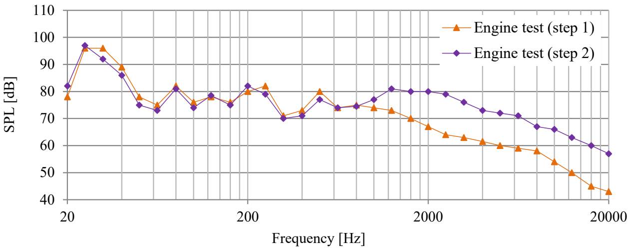

Fig. 13. Measured SPL inside the cabin; the engine test (steps 1 and 2).

Figure 14 shows the SPL inside the cabin for the engine test (steps 2 and 4). For the frequencies above 1000 Hz, coverage of the floor with the sound barrier effectively reduces the SPL inside the cabin. An average reduction of 17 dB is observed in the SPL inside the cabin. However, coverage of the floor with acoustic materials does not affect the cabin noise reduction for the frequencies lower than 1000 Hz. The engine noise is transmitted into the cabin by the structure itself in this frequency range.

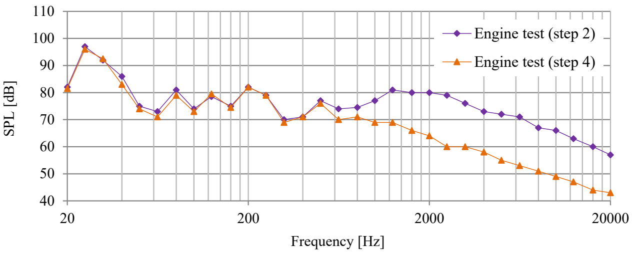

Fig. 14. Measured SPL inside the cabin; the engine test (steps 2 and 4).

Figure 15 shows the measured SPL inside the cabin for the road test (steps 1, 5, and 6) in dBA. The overall noise level at the microphone position decreases from 80 to 70 dBA. The final value is mainly influenced by the peak of acoustic energy in the frequency band of 250 Hz, a frequency component related to the engine rotation. In order to obtain a further reduction of the overall dBA level, it will be necessary to investigate this peak first, probably due to some structure-born vibration. Foam injection has a relatively good effect at low frequencies.

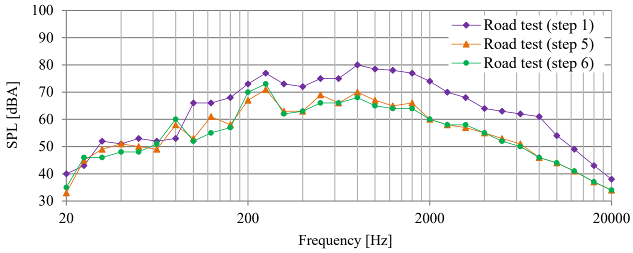

Fig. 15. Measured SPL inside the cabin; the road test (steps 1, 5, and 6) in dBA.

5. Conclusions

Investigations were made to control the MB truck cabin interior noise by reducing noise in the transmission path. A viscoelastic layer damping material was used to reduce the vibration amplitude of the cabin back wall. Computational results were then compared with the values obtained by the experimental modal analysis results. Good agreement was found between the theoretical and experimental results. A sound barrier, silicon adhesive, and foam were utilised for noise control in the transmission path. The effectiveness of the mentioned acoustic materials on cabin noise reduction was experimentally evaluated. The measurements focused on carpet impact, coverage of leaks in the firewall (by sound barriers and silicon adhesive), and floor coverage (by sound barriers). By looking at the graphs, it is possible to understand the influence of the different trim parts and the modifications made, but it is also interesting to see the peaks in the spectra. Those peaks are probably related to the presence of excited acoustic modes, and this phenomenon should be investigated to verify this. The excitation of acoustic modes in acoustic cavities of the vehicle by the engine running is a common problem in noise reduction. However, it requires specific investigations and acoustic modelling to understand what can be done.

The loudspeaker test results show that the carpet impact, coverage of leaks in the firewall by the sound barrier and silicone adhesive, and coverage of the floor by the sound barrier have a significant effect on the cabin noise reduction for the frequencies above 1000 Hz. For the frequencies lower than 1000 Hz, a significant portion of the noise is transmitted into the cabin by the structure itself; therefore, those treatments do not reduce cabin noise.

The engine test results show that the coverage of the firewall leaks does not affect the cabin noise reduction. It seems that the engine noise is still transmitted into the cabin by the structure itself (structure-borne noise). However, for the frequencies above 1000 Hz, the carpet and coverage of the floor have a significant effect on the cabin noise reduction. For the frequencies lower than 1000 Hz, those treatments do not affect the cabin noise reduction.

The road test results show that a complete treatment, including the coverage of the floor and firewall leaks by acoustic materials and silicone adhesive and foam injection into the side member, has a significant effect on the cabin noise reduction. The overall noise level at the microphone position decreases from 80 to 70 dBA. The final value is mainly influenced by the peak of acoustic energy in the frequency band of 250 Hz, a frequency component related to the engine rotation. In order to obtain a further reduction of the overall dBA level, it will be necessary to investigate this peak first, probably due to some structure-born vibration. Foam injection has a relatively good effect at low frequencies.

References

1. Ang L.Y.L., Koh Y.K., Lee H.P. (2016), Acoustic metamaterials: a potential for cabin noise control in automobiles and armored vehicles, *International Journal of Applied Mechanics*, **8**(5), doi: 10.1142/S1758825116500721.
2. Antila M., Hao Y., Lankila A., Yu J. (2008), Possibilities and benefits of active noise control (ANC) in truck cabins, [in:] *Proceedings: 37th International Congress and Exhibition on Noise Control Engineering, INTER-NOISE 2008*, **1**: 444–449, Shanghai, China.
3. Barber A. (1992), *Handbook of Noise and Vibration Control*, 6th ed., Elsevier Science, Oxford.
4. Bealko S.B. (2009), Mining publication: Mining haul truck cab noise: An evaluation of three acoustical environments, *The National Institute for Occupational Safety and Health (NIOSH)*, **61**(10): 36–42.
5. Beranek L.L. (1992), *Noise and Vibration Control*, John Wiley.
6. Harris C.M. (1991), *Handbook of Acoustical Measurements and Noise Control*, 3rd ed., McGraw-Hill, New York.
7. ISO 5128 Standard (1980), *Acoustics-Measurement of Noise Inside Motor Vehicles*.
8. Johnson E. (1996), *Tires and Handling*, Society of Automotive Engineers.
9. Jones D.I.G. (1985), *Damping Materials for Vibration & Sound Control*, John Wiley, New York.
10. Li H.B., Liu H.G., Liu J.C., Shangguan Y.F. (2008), Active noise control of the heavy truck interior cab, *Journal of Beijing Institute of Technology*, **17**(4): 400–404.
11. Lu Q.C., Li H.B., Huang H. (2013), Simulation of active noise control system on the truck interior cab, *Advanced Materials Research*, **798–799**: 443–447, doi: 10.4028/www.scientific.net/AMR.798-799.443.
12. Malik A.K. (1990), *Principle of Vibration Control*, Affiliated East-West Press, India.
13. Mohanty A.R., Pierre B.D., Suruli-Narayanasami P. (2000), Structure-borne noise reduction in a truck cab interior using numerical techniques, *Applied Acoustics*, **59**(1): 1–17, doi: 10.1016/S0003-682X(99)00018-3.
14. Nashif A.D., Jones D.I.G., Henderson J.P. (1985), *Vibration Damping*, John Wiley, New York.
15. Pujara K. (1992), *Vibration & Noise for Engineers*, 4th ed., Dhanpat Rai & Sons, Delhi.
16. SAE-J336 Standard (2011), *Sound Level for Truck Cab Interior*, SAE International.
17. Saxena S., Jadhav S. (2021), Truck front cabin mount tuning for cabin noise boom, overall interior noise and vibration reduction, [in:] *Symposium on International Automotive Technology*, Pune, India, doi: 10.4271/2021-26-0286.
18. Society of Automotive Engineers (SAE) (1992), *Truck Systems Design Handbook*, Society of Automotive Engineers.
19. Taylor C.F. (1982), *The Internal Combustion Engine in Theory and Practice*, Vol. 2, 5th ed., Massachusetts Institute of Technology.